Journal of Membrane Science 526 (2017) 181–190

Contents lists available at ScienceDirect

Journal of Membrane Science

journal homepage: www.elsevier.com/locate/memsci

Evaluation of a novel physical cleaning strategy based on HF membrane rotation during the backwashing/relaxation phases for anaerobic submerged MBR

Ignacio Ruigómez, Enrique González, Sonia Guerra, Luis E. Rodríguez-Gómez, Luisa Vera*

Departamento de Ingeniería Química y Tecnología Farmacéutica, Facultad de Ciencias, Sección de Química, Universidad de La Laguna, Avenida Astrofísico Francisco Sánchez, s/n. Campus de Anchieta. Apdo. de correos 456, 38200 La Laguna, Tenerife, Spain

ARTICLE INFO

Keywords:
Anaerobic membrane bioreactor
Membrane rotation
Transmembrane set-point
Fouling
Hollow fibre
Gas scouring

ABSTRACT

A novel physical cleaning strategy based on membrane rotation was investigated in an anaerobic membrane bioreactor treating wastewater. This strategy was proposed to improve the fouling removal effectiveness of the traditional physical cleaning techniques (such as backwashing and relaxation) by the shear-enhanced conditions associated with the rotation. The effectiveness of this strategy has been investigated in a bench filtration unit during short-term tests and also compared to the conventional mode with gas scouring. Based on the resistances-in-series approach, the external residual fouling has been identified as the main factor determining the process productivity. The contribution of this type of fouling obtained with the rotating membrane was lower than with the gas scouring application (56–18% versus 60–53%, respectively). Other operational parameters such as the transmembrane pressure set-point for cleaning initiation and the backwashing time have also showed a significant influence on external fouling re-dispersion. A long-term test revealed the sustainability of the operation during more than 400 h, achieving a stable net permeate flux of 6.7 L/h m^2 when the rotating speed was fixed in 340 rpm.

1. Introduction

Nowadays, anaerobic membrane bioreactors (AnMBRs) have been identified as an emerging technology with a great potential in the field of domestic wastewater (DWW) treatment and reuse. Unlike conventional aerobic membrane bioreactors, AnMBRs allow energy recovery by conversion of organic matter into methane-rich biogas during the anaerobic digestion. In addition, the overall energy consumption is reduced because no aeration energy is required for mineralizing the DWW organics [1,2]. Membrane filtration also solved the operational and biological issues associated to the classical anaerobic schemes, where gravity separation is usually employed to split up the water product from the anaerobic suspension. Thus, AnMBRs avoid the biomass to be washed out from the reactor, producing a high quality effluent without particulate matter. Besides, hydraulic retention time (HRT) is separated from the solids retention time (SRT), favouring the slow growth of the anaerobic microorganisms at ambient temperatures [3,4]. Another key factor of AnMBRs is the presence of high contents of nitrogen and phosphorus in the effluent, enabling its direct use for irrigation, and the opportunity to recover nutrients from the wastewater [5].

However, despite AnMBRs emerge as a promising technology, membrane fouling currently remains being one of its major drawbacks, reducing the membrane permeability, shortening the membrane lifespan and increasing the cleaning frequency [1–4]. It is known that anaerobic suspensions are a complex mixture of biomass, colloidal particles, soluble organics and inorganic precipitates [4]. Unlike aerobic MBRs, which typically operate with permeate fluxes ranged between 20–30 L/h m^2 [6], the higher concentrations of solids and non-settleable matter present in submerged AnMBRs lead to a greater fouling membrane propensity. In fact, it limits the operational permeate fluxes to values between 5–12 L/h m^2 [2]. Hence, the choice of the appropriate cleaning strategy plays a key role on the sustainability and economic feasibility of the AnMBR operation. Physical cleanings, such as relaxation (temporary interruption of permeate filtration) and backwashing (use of permeate to flush the membrane backwards), are usually employed to remove reversible fouling, which is usually related to the detachment of a cake layer weakly bounded to the membrane surface. However, when physical cleaning is not optimised, the system cannot completely disperse the detached cake, resulting in a

* Corresponding author.
E-mail addresses: isempere@ull.edu.es (I. Ruigómez), eglezc@ull.es (E. González), sonia.-94@hotmail.com (S. Guerra), luerguez@ull.es (L.E. Rodríguez-Gómez), luvera@ull.es (L. Vera).

http://dx.doi.org/10.1016/j.memsci.2016.12.042
Received 3 October 2016; Received in revised form 19 December 2016; Accepted 20 December 2016
Available online 22 December 2016
0376-7388/

Nomenclature

AnMBR	anaerobic membrane bioreactor
COD	chemical oxygen demand, mg/L
d_{50}	diameter corresponding to 50% of cumulative undersize, μm
DOC	dissolved organic carbon, mg/L
dv/dr	shear rate, s^{-1}
DWW	domestic wastewater
GS- HFM	gas-sparging hollow fibre membrane
HF	hollow fibre
HRT	hydraulic retention time
IA	intermediate alkalinity, mg $CaCO_3$/L
IA/TA	alkalinity ratio
J	permeate flux, L/h m^2
J_B	backwashing flux, L/h m^2
J_{net}	net permeate flux, L/h m^2
m	consistency index, mPa·s
MBR	membrane bioreactor
MLSS	mixed liquor total suspended solids, g/L
MLVSS	mixed liquor volatile suspended solids, g/L
n	flow behaviour index
PSD	particle size distribution
Q_g	gas flow-rate, m^3/s
r_f	cake fouling rate, kPa/s
R_{ef}	external residual fouling resistance, m^{-1}
R_{if}	internal residual fouling resistance, m^{-1}
R_m	clean membrane resistance, m^{-1}
R_{rdf}	residual fouling resistance, m^{-1}
R_{rvf}	reversible fouling resistance, m^{-1}
R_{sp}	total hydraulic resistance related with the transmembrane pressure set-point, m^{-1}
R- HFM	rotating hollow fibre membrane
SGD	specific gas demand, $m^3/h{\cdot}m^2$
SRT	solids retention time
t_B	backwashing phase duration, s
t_F	filtration phase duration, s
t_R	relaxation phase duration, s
TA	total alkalinity, mg $CaCO_3$/L
TMP	transmembrane pressure, kPa
TMP_O	transmembrane pressure associated with residual fouling phenomena, kPa
TMP_i	initial transmembrane pressure after backwashing, kPa
TMP_{sp}	transmembrane pressure set-point, kPa
TSS	total suspended solids, g/L
TTF	time-to-filter, s
VFA	volatile fatty acids
w	rotating speed, rpm
WWTP	wastewater treatment plant

Greek letters

Θ_B	net backwashing ratio
μ	permeate viscosity, Pa s
μ_a	apparent viscosity, Pa s

foulants accumulation in the membrane vicinities. Therefore, when the filtration restarts at the subsequent filtration cycle, these foulants collapse back quickly on the membrane surface [7]. This new fouling contribution is known as external residual fouling [8]. By contrast, chemical cleanings are required to remove internal residual fouling caused by pore narrowing or blocking and strongly attached layers (e.g. gel or dense cakes) during membrane filtration [9].

On the other hand, exploring dead-end operation, that offers the potential of lower energy demands (filtration is performed without shear forces), seems to be an attractive option to save costs. Recently, Vera et al. [10] have demonstrated the feasibility of an aerobic submerged membrane bioreactor operated in dead-end mode at moderate biomass concentrations (4–8 g/L). Nevertheless, due to the complex nature of the anaerobic suspensions, its applicability to AnMBRs will be conditioned to an effective control of cake removal by physical cleanings, which has been identified as the major contribution to membrane fouling [11]. Relaxation and backwashing combinations are usually applied in AnMBRs systems [12,13], whose efficiency can be further increased with the aid of shear promoters [14–16]. Even so, optimal operating conditions depend on each particular system characteristics which has driven the development of dynamic feedback control systems [17]. Physical cleanings initiation by a preselected transmembrane pressure set point (TMP_{sp}) allows the system to adjust automatically the filtration time and, therefore, the physical cleaning frequency as a function of the fouling extent. A recent study performed with anaerobic suspensions demonstrated the high effectiveness of this control system (92.7 ± 2.2%) in preventing residual fouling even at high fluxes [18]. Therefore, this cleaning operation mode allows increasing the filtration time and the cleaning efficiency, enhancing thus, the process productivity [19].

As previously stated, the use of shear promoters during the backwashing/relaxation periods could be an attractive option to improve the physical cleaning. Gas sparging is widely employed in AnMBRs by biogas recirculation. The shear rates generated by the rising bubbles promote the detachment and the re-dispersion of the loose cake layer, favouring the mass transport [20]. However, several studies confirmed the existence of a threshold gas-sparging intensity beyond which further increases have no benefit on fouling mitigation [21,22]. In addition, gas scouring effectiveness can be reduced by high biomass concentrations and viscosities [23], typical of the anaerobic mixed-liquors, and the preference of gas bubbles to flow through low resistance paths (e.g. membrane sides) [24]. On the other hand, new insights focused on dynamic shear-enhanced membrane systems, such as rotating or vibrating systems, highlight the advantages of employing a moving part to create the shear forces. Hence, more energy is focused on the membrane cleaning and less is dissipated in the bulk suspension [16]. Unlike the first designs based on ceramic concentric tubes, rotating hollow fibre membranes (R-HFM) present high specific surfaces and are economically competitive [25]. Several studies have found that the flux increases with the rotating speed as a result of the greater shear forces [26,27]. In fact, the shear forces generated by R-HFMs are able to generate uniform gradients in the axial direction, enhancing the overall mass transfer [28]. Also, a recent AnMBR study conducted at pilot scale with a R-HFM suggested that module rotation not only can limit the foulants deposition, but also detach the cake layer formed during the filtration stage in absence of permeate flux [29].

The main objective of this paper was to evaluate a novel physical cleaning strategy to limit membrane fouling based on a hollow fibre membrane rotation during the physical cleaning phases. The analysis of the system performance was accomplished through short-term filterability tests for assessing the influence of several operational conditions (rotating speed, transmembrane set-point and backwashing time). These results were compared with those obtained with a gas scouring module. Finally, process sustainability was analysed during long-term operation.

2. Material and methods

2.1. Bench scale AnMBR

2.1.1. Configuration for filtration tests

The AnMBR was configured as a filtration unit and operated in a closed loop, through a stirred 3 L tank for the filtration tests. The unit allows operating with two different PVDF hollow-fibre modules: a conventional gas-sparging membrane (GS-HFM) and a rotating membrane (R-HFM). Both membrane modules have an average pore size of 0.04 μm and a nominal membrane surface area of 0.047 m^2 (GE Water & Process Technologies, USA). A detailed description of the membrane modules can be found in Ruigómez et al. [27]. Permeate was withdrawn at constant flux (J) from outside to inside the fibre through the vacuum created by a magnetic drive gear pump (Micropump-GA Series, USA). A magnetic stirrer (100 rpm) located at the bottom of the tank was used to ensure anaerobic suspension homogeneity. Membrane fouling was evaluated as a function of the transmembrane pressure (TMP) evolution, registered by a pressure sensor (Sensotech, Spain). To maintain process productivity, traditional strategies for fouling mitigation such as physical cleaning techniques (backwashing or relaxation) have been applied. However, in this paper the efficiency of these physical cleanings was improved with the aid of different turbulence promoters according to module configuration. In the conventional GS-HFM module, N_2 was supplied through an extended aeration tube located inside the membrane module to promote shear rate and move the fibres. The gas flow-rate was established and measured by a mass flow controller (Bronkhorsts®-EL-FLOW, the Netherlands). In contrast, in the R-HFM configuration, the gas feed conduit was replaced by a mechanical stirrer (Heidolph-RZR2020, Germany) connected to the permeate line, which was the impeller of membrane rotation. For both modules, the initiation of the cleaning phases was controlled by a transmembrane pressure set-point (TMP_{sp}), according to previous studies [27].

DAQ Factory software (AzeoTech®, Inc., USA) was employed to control the unit and acquire the data. The control system software allows setting J, TMP_{sp}, and the main physical cleaning variables: relaxation and backwashing times (t_R and t_B, respectively) and backwashing flux (J_B).

2.1.2. Configuration for continuous operation

The bench scale AnMBR was adapted from the filtration test unit with the R-HFM to operate in continuous mode (Fig. 1). Three peristaltic pumps Masterflex Easy-Load L/S 7518-00 (Cole-Parmer Instrument Co., USA), two level controllers HSE-20987 (Aeman, Spain) and an 8 L feed wastewater tank were added to the original scheme. The bioreactor was equipped with a hydraulic seal in order to prevent the entrance of environmental oxygen and to allow the membrane module rotation. The peristaltic pump P-1 fed the wastewater from the 8 L tank to the AnMBR by the action of the level controller LC-1. The level of the anaerobic suspension was adjusted to remain always above the seal. In addition, the peristaltic pumps, P-3 and P-4, were employed to keep the HRT constant, removing part of the effluent from the permeate tank and recirculating the rest into the bioreactor. The level controller LC-2 ensured a minimum level of effluent in the permeate tank in order to carry out periodical backwashing cleanings. The laboratory AnMBR was run at ambient temperature (17.3 ± 1.5 °C) and the HRT was kept at 31 h, the same value of the pilot-scale AnMBR that supplied the anaerobic suspensions for the filterability trials. Also, no sludge removal took place along the experimental period, except for sampling.

2.2. Experimental operation

2.2.1. Short-term filtration tests

For the short-term tests, the bench scale unit was fed with fresh anaerobic suspensions from a pilot-scale AnMBR located in the wastewater treatment plant (WWTP) of Valle Guerra (Tenerife, Canary Islands, Spain). The experimental conditions of the pilot plant were kept constant (hydraulic and solids retention times were 31 h and 116 d, respectively). The anaerobic suspensions were characterised before each test to ensure the reproducibility of experiments, as well. The Table 1 summarises the average values of the significant parameters.

Suspensions presented typical values of biomass concentration and median particle size (MLSS=10.8 g/L and d_{50}=28.9 μm), and comparable to those reported in other AnMBR studies [18,30]. Consistently, moderate values of time to filter (TTF=11.8 min) and supernatant turbidities (2545 NTU) were also reported. As expected, the apparent viscosity of the sludge was reduced with the shear intensity. According with previous studies [31], the rheological behaviour can be described by the non-Newtonian Ostwald-de-Waele model:

$$\mu_a = m \cdot \left(\frac{dv}{dr}\right)^{n-1} \quad (1)$$

where μ_a is the apparent viscosity, dv/dr is the shear rate, n is the flow behaviour index and m is the consistency index.

2.2.2. Long-term filtration test

The AnMBR was continuously fed with screened (2 mm step), degritted, degreased and settled domestic wastewater from the WWTP of Valle Guerra (Fig. 1). The feedwater was characterised three times per week through the whole experimental period. Table 2 summarises the average values of the inlet properties. The domestic wastewater exhibited comparable contents in total suspended solids (TSS) and chemical oxygen demand (COD) to those reported in similar studies [32], where soluble COD fraction represents 61% of total COD. pH of the wastewater remained constant during the operation with values around 7.9 ± 0.2. At the same time, the influent presented typical DWW ammonium and phosphate concentrations [33] and low sulphate content [34].

2.3. Analytical methods

Chemical oxygen demand (COD), dissolved organic carbon (DOC), total suspended solids (TSS), mixed-liquor total suspended solids (MLSS), mixed-liquor volatile suspended solids (MLVSS) and pH were determined according to the Standard Methods [35]. The standard method 2710-H, called as “time to filter” (TTF), was adapted for anaerobic suspensions. This modification involved measuring the time required to filter 50 mL of sludge through a WHATMAN 934 AH glass-

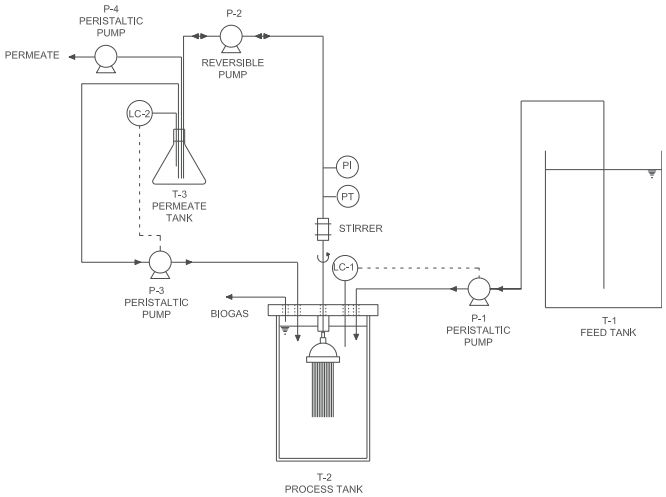

Fig. 1. Configuration of the bench scale AnMBR.

Table 1
Main characteristics of suspensions employed to perform the short-term experimental trials.

Parameter	Unit	Mean	Standard deviation	Range	n
MLSS	g/L	10.8	1.0	9.1–11.9	9
MLVSS	g/L	8.3	0.8	7.1–9.8	9
d_{50}	μm	28.9	1.0	27.9–30.1	5
TTF	min	11.8	0.7	10.7–12.6	6
Supernatant turbidity	NTU	2545	589	1705–3355	5
m	mPa s	24.1	2.0	21.5–26.0	6
n		0.63	0.03	0.58–0.65	6

Table 2
Main characteristics of the DWW fed to the bench scale AnMBR.

	Unit	Mean	Standard deviation	Range	n
TSS	g/L	0.09	0.03	0.06–0.16	8
COD	mg/L	381	104	251–583	8
COD_s	mg/L	233	51	189–344	8
$N\text{-}NH_3$	mg/L	66.8	7.1	60.6–81.7	8
$P\text{-}PO_4$	mg/L	9.1	0.8	8.0–10.1	7
$S\text{-}SO_4$	mg/L	10.3	2.6	6.7–13.7	6
pH		7.9	0.2	7.6–8.1	9

fibre filter, to obtain 15 mL of sample. Supernatant turbidity was quantified after centrifuging the suspension samples at 3000 g for 2 min. Sludge particle size distribution was measured with the Malvern Mastersizer 2000 through the small volume entry level wet dispersion unit, Hydro 2000 SM (Malvern Instruments Ltd., UK). Total alkalinity (TA) and intermediate alkalinity (IA) were determined through titration [35]. IA is usually associated to volatile fatty acids (VFA) [36] and alkalinity ratios (IA/TA) higher than 0.3 indicates VFA accumulation. Nessler method [35] and HACH reagents were employed to determine ammonia nitrogen. Ion chromatography was employed in order to determine phosphate and sulphate concentrations (PO_4^{3-} and SO_4^{3-}) using the Methrom 882 Compact Ion Chromatograph instrument (Methrom, Switzerland).

2.4. Membrane fouling characterisation

According to previous studies [8], membrane fouling has been analysed by the resistance-in-series model. Therefore, at the beginning of the filtration phase, the initial *TMP* (TMP_i) can be related to two different resistances, as expressed in Eq. (2):

$$TMP_i = J \cdot \mu \cdot (R_m + R_{if}) \quad (2)$$

where J is the permeate flux, μ is the permeate viscosity, R_m is the pressure associated to the hydraulic membrane resistance and R_{if} is the resistance originated by the internal residual fouling, which is not removed through physical cleanings. In addition, two different stages appear during the filtration phase: an initial sharp *TMP* increase followed by a slow linear increase. The first increase can be attributed to a severe membrane fouling due to a cake pre-deposition process, as previously reported [8,41]. This phenomenon is assumed to be caused by the foulants detached from the membrane during the previous physical cleaning which are not completely dispersed away from the convective zone near the membrane surface. Then, at the beginning of the subsequent cycle, the displaced cake was rapidly deposited on to the membrane originating the quick *TMP* increase up to a characteristic value (TMP_O). This value, which among other factors, mainly depends on the physical cleaning efficiency [8], can be related to the residual fouling phenomena (R_{rdf}):

$$TMP_0 = J \cdot \mu \cdot (R_m + R_{rdf}) = J \cdot \mu \cdot (R_m + R_{if} + R_{ef}) \quad (3)$$

where R_{ef} is the external residual fouling resistance. Beyond TMP_O, the *TMP* evolution with the elapsed time followed a linear trend, which suggests a cake formation mechanism:

$$TMP = TMP_0 + r_f \cdot t \quad (4)$$

where the slope of the straight line is defined as the fouling rate (r_f), which is usually employed to quantify the membrane fouling. Finally, when the *TMP* reaches the set-point value (TMP_{sp}), the total hydraulic resistance R_{sp} can be defined by Eq. (5):

$$TMP_{sp} = J \cdot \mu \cdot R_{sp} = J \cdot \mu \cdot (R_m + R_{rdf} + R_{rvf}) \quad (5)$$

where R_{rvf} is the reversible fouling resistance.

2.5. Membrane cleanings

2.5.1. Analysis of the fouling layer removed by the physical cleanings

A specific experimental procedure was developed in order to quantify the foulants removed by the physical cleaning. First, a clean membrane was submerged in the microbial suspension and it was fouled until reach the TMP_{sp} by filtering at 8 L/h m^2 (i.e. reproducing a filtration cycle of the short-term tests). Then, the fouled membrane was taken off and submerged in a 3 L tank with Milli-Q water where a physical cleaning was carried out at similar operating conditions (J_B, t_B, t_R and rotating speed) as employed during the short-term assays. Finally, at the end of the cleaning phase, a sample of bulk solution (i.e. removed foulants suspended in Milli-Q water) was taken to be analysed in terms of MLSS and DOC.

2.5.2. Membrane cleaning protocol for fouling fractionation

Fouling fractionation is widely used to provide further understanding of the fouling layers contribution [16,37,38]. After the long-term test the fouled membranes were cleaned “ex-situ” following a specific protocol that included the following four steps: (1) rinsing with 1.2 L of Milli-Q water; (2) extended backwashing with a flux of 30 L/hm^2 with 1.2 L of Milli-Q water; (3) desorption by chemical cleaning with a 1.2 L solution of sodium hypochlorite (500 mg/L) for 24 h; (4) desorption by chemical cleaning with a 1.2 L solution of citric acid (6000 mg/L) for 2 h. After each step, clean water filtration test was applied to measure the remaining resistance of each fraction: rinsed, backwashed, desorbed with NaOCl and desorbed with citric acid. Whilst the physical steps (rinse and extended backwash) are expected to remove the external residual fouling, which is related to the foulants/cake layer that remains on the membrane surface at the end of the experimental assays (i.e. fouling which cannot be removed by the conventional physical cleanings performed “in-situ”), the resistance recovered from the chemical steps (NaOCl and citric acid desorption) is linked with the internal residual fouling (gel layer formation or pore narrowing).

3. Results and discussion

3.1. Short-term filtration tests

3.1.1. Comparison of rotating and gas-sparging modules

Short-term tests with two modes for inducing shear stress during the physical cleaning phase, using the two different modules (GS-HFM and R-HFM), were conducted to evaluate their impact over the membrane fouling. Fig. 2 shows an example of the filtration cycle time evolution (t_F) during the filtration tests. In both cases, filtration cycles were shortened with the operation time until reach a pseudo-stationary zone. This dynamic trend is typical of systems controlled by TMP_{sp} backwashing initiation and operated at constant permeate flux [19]. At the beginning of the test, as a result of permeate driving force, foulants were gradually deposited onto the fibres and consequently, the *TMP* increased. Once reached a set-point value, the physical cleaning started and the deposits were partially detached and re-dispersed to the bulk suspension. Consequently, the control system dynamically adjusts the physical cleanings frequency accordingly to the membrane module

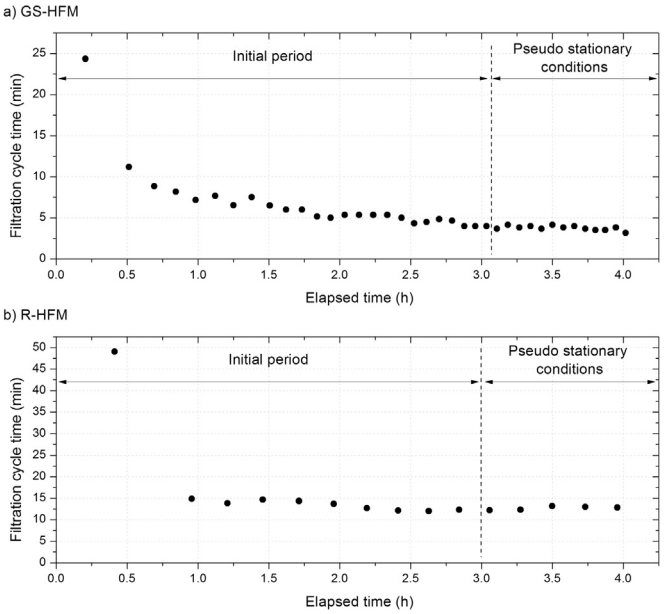

Fig. 2. Filtration cycle time (t_F) evolution with the elapsed time for the two different membrane modules: (a) gas scouring membrane (GS-HFM) and (b) rotating membrane (R-HFM). J=8 L/h m^2; TMP_{sp}=30kPa; Backwashing; J_B=30 L/h m^2; t_B=30 s; Q_g=2 NL/min; w=180 rpm.

fouling extent. Thus, the deposited and removed matter was progressively compensated until the system was well balanced. After this equilibrium point, the filtration length remained nearly constant during the successive cycles (i.e. the pseudo-stationary zone). However, it must be noted that higher times were required to stabilise the filtration cycles in systems with a lower cleaning efficiency. This can be clearly observed in the Fig. 2, where the GS-HFM reached the pseudo-stationary zone later than the R-HFM. Nevertheless, in this work, the pseudo-stationary zone was defined after 3 h of operation, when the systems showed a relative stable behaviour for all the tested conditions. By comparing filtration cycle times (t_F) of both configurations, it can be observed higher values for the *R-HFM*, revealing a better fouling control. This issue will be further discussed in the following sections. In addition, the differences observed for the initial t_F values may be related to the absence of the lower header in the *R-HFM* configuration. As a consequence, the slight turbulence employed for mixing the bulk suspension may have a higher effect in fouling prevention (i.e. by increasing shear forces and fibre movement degree) in the *R-HFM*. Nevertheless, this phenomenon seems to be less significant as the filtration proceeds and the physical cleaning strategies employed become more important for fouling control.

Fig. 3 compares the filtration *TMP* profiles, obtained in the pseudo-stationary zone, for both modules at different shear conditions. Five gas flow rates (Q_g) and six rotating speeds (w) were tested during the backwashing phase (J_B=30 L/h m^2;t_B=30 s) as physical cleaning strategies. All the trials were carried out under the same filtration conditions (dead-end mode, J=8 L/h m^2 and TMP_{sp}=30 kPa). In agreement with previous studies [8], two different stages can be identified in each one of the *TMP* profiles during the filtration cycles for both modules. In the first phase, a sharp *TMP* increase took place up to TMP_O as a consequence of the rapid pre-deposition of the detached matter that could not be re-dispersed through the physical cleanings. Then, during the second stage a slow linear rise was observed, associated to a new cake layer formation.

As expected, filtration length increased with the shear stress induced by gas-sparging or rotating speed, consistently with the approach based on cake re-dispersion. However, the extent of the re-dispersion phenomenon due to gas scouring seems to be lower than that achieved through membrane module rotation. It should be noted that in submerged HF modules with gas scouring, shear stress profiles are highly spatially and temporally variable [39]. Hence, this non homogeneous shear distribution may limit dispersion efficiency, potentially resulting in zones with lower shear forces. Indeed, in the present study it was possible to observe a boundary flow rate at 2 NL/min (SGD_m=0.3 m^3/h m^2), above which there was no appreciable improvement of fouling control (Fig. 3a). At this boundary value, the maximum filtration length that can be obtained was 3.7 ± 0.3 min. A similar trend was reported by McAdam et al. [40] for a submerged HF MBR operated in dead-end mode with periodical filtration/backwashing cycles. These authors observed that beyond a certain value, ranged between 0.67 and 1.5 depending on the filtered volume, an increase in the gas flow rate during the backwashing phase did not led to lower values of fouling rates. According to these authors, experimental results seem to indicate that shear controls the matter remaining in the convective zone rather than providing deposit reversibility.

In contrast, when the R-HFM configuration was employed (Fig. 3b), all fibres were expected to be subjected to the shear forces associated to the module rotation during the physical cleanings. Nevertheless, results suggest the existence of a threshold value (60 rpm) below which membrane rotation did not improve the backwashing efficiency. Thus, comparable filtration cycles were obtained when physical cleaning was carried out with w values of 0 and 60 rpm. This behaviour may be attributable to the fact that the turbulence generated in the membrane vicinities is too low to disperse the deposited matter, which is in accordance to previous results [27]. Above this threshold value, the higher rotating speed, the greater matter re-dispersion and, consequently, the larger filtration times. In fact, when the physical cleaning was aided with a membrane rotation at 340 rpm, the filtration length was similar than that obtained at the beginning of the test with a clean membrane (40.0 and 42.7 min, respectively). This suggested that almost complete matter re-dispersion took place at this rotating speed,

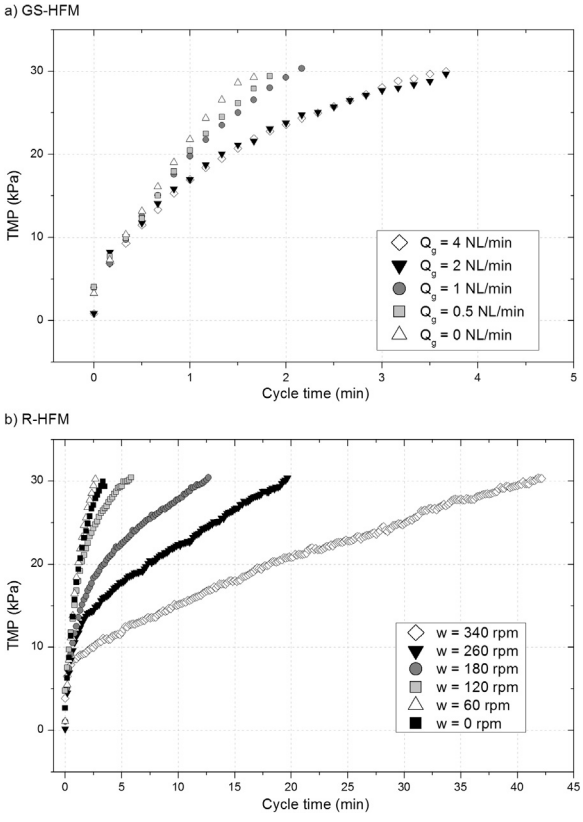

Fig. 3. TMP profile corresponding to a filtration phase at different gas flow rates or rotating speeds for (a) GS-HFM and (b) R-HFM. Pseudo-stationary zone; J=8 L/h m^2; Backwashing; J_B=30 L/h m^2; t_B=30 s; TMP_{sp}=30kPa.

which allows to achieve filtration durations 10 times greater than those obtained with gas sparging.

Fig. 4 shows the relative contribution of the different fouling resistances to the hydraulic resistance at the TMP_{sp} (i.e. at the end of the filtration phase) according to the resistances in-series model (Eq. (5)). Results showed a slight experimental deviation on the R_m contribution (11–19%) which may be associated to the chemical cleaning efficiency achieved before each one of the short-term filterability tests. As mentioned before, the low internal fouling obtained (R_{if}) may be attributed to the dead-end filtration conditions applied (i.e. absence of shear forces during the filtration phase), where particles and colloids are freely moved toward the membrane [8,40]. Consistently, the main contribution to the total resistance was the external matter deposition (R_{rvf}+R_{ef}), with percentages ranged between 75% and 80% of the total hydraulic resistance, regardless of the module configuration employed. Particularly relevant is the contribution of the external residual fouling (R_{ef}), which varied according to the shear forces induced by gas flow rate or the rotating speed, since it is the main determining factor on filtration length due to the quick development of this type of fouling. In fact, in absence of shear forces, the R_{ef} account for more than 70% of the total hydraulic resistance for both configurations (Fig. 4). For the GS-HFM, R_{ef} slightly decreased from 73% to 52% as Q_g increased from 0 to 2 NL/min (Fig. 4a). Above this value, the R_{ef} seemed to remain nearly constant, suggesting that the system was not able to increase this level of cake re-dispersion. In contrast, R-HFM produced a linear decrease in the R_{ef} values until achieve very low values (18% of the total hydraulic resistance) when a rotating speed of 340 rpm was applied (Fig. 4b). This high efficiency in cake re-dispersion may be the main reason for the very large filtration lengths observed at high w (Fig. 3b).

In order to quantify the dispersed matter by the action of the rotating speed in the R-HFM, additional tests were conducted. In these tests, a fouled membrane (once reached the TMP_{sp}) was taken off and submerged in Milli-Q water where the physical cleaning was carried out. Fig. 5 shows the dispersed matter, determined in terms of the suspended solids and micro-colloidal/soluble organics (expressed by DOC), against w. It can be observed that solids removed varied from 0.9 g/m^2 to 4.6 g/m^2 whilst DOC concentrations ranged from 56.1 to 78.2 mg/m^2, for w values between 0 and 340 rpm, respectively. These results support the cake re-dispersion approach, where large particles (i.e. suspended solids) were mainly responsible for the external residual fouling.

3.1.2. Effect of combining backwashing and relaxation during physical cleaning in the R-HFM

The role of rotating speed in membrane fouling had previously been attributed to the shear stress induced on the membrane surface, re-dispersing the cake layer detached from the membrane during the backwashing. This section investigates the effect of combining backwashing and relaxation during the physical cleaning period with the aim of reducing the backwashed volume and thus, the loss of productivity. For this purpose, the net backwashing ratio (Θ_B) has been defined by Eq. (6):

$$\theta_B = \frac{t_B}{t_B + t_R} \quad (6)$$

where t_B is the backwashing time and t_R is the relaxation time during a cycle.

All the tests were performed with the same overall cleaning duration (t_B+t_R=30 s) at moderate rotating speed (180 rpm). At this w value (in accordance with the results obtained in the previous section) similar cycle times (t_F=12.7 min) to those usually employed in full scale municipal WWTPs equipped with HF MBRs (10 min) were obtained [6]. Permeate and backwashing fluxes were fixed at 8 and 30 L/hm^2, respectively, and two different TMP_{sp} (20 and 30 kPa) were applied. It must be noted that when both physical cleaning methods were coupled, backwashing was always employed in first place, followed by relaxation.

Fig. 6 displays the relative contribution of the different hydraulic resistances against Θ_B at two TMP_{sp} values. For the internal residual fouling (R_{if}), it can be observed that the effectiveness of Θ_B on fouling control could be separated in two zones. When Θ_B is 0 (i.e. only relaxation was applied), there was a substantial effect on the internal fouling by TMP_{sp}, resulting in a significant contribution at the highest value (30 kPa), probably due to a considerable cake consolidation as previously reported [19]. Nevertheless, when the net backwashing ratio was increased ($\Theta_B \geq 0.33$) a clear tendency was not observed, resulting in a low R_{if} contribution (8–15%) regardless of the applied conditions. It is assumed that most of the cake was effectively detached from the membrane, whatever the selected TMP_{sp} (i.e. the degree of membrane fouling achieved). Concerning the external residual fouling (R_{ef}), the relative contribution decreased with increasing Θ_B but this effect was less significant at the highest TMP_{sp}. This may be related to the thickness of the cake layer on the membrane surface, which increased with the TMP_{sp} due to the extension of the filtration phase [41]. Therefore, it is reasonable to assume that for given cleaning conditions, the amount of cake remaining in the convective zone near the membrane (i.e. not dispersed) increases with the TMP_{sp}. These results highlighted the important role played by the backwashing, which not only contributed to prevent the internal membrane fouling, but also to favour cake layer detachment, improving the foulants dispersion by the action of the shear forces. Nevertheless, at the lower TMP_{sp}, a value of 0.67 for the Θ_B seemed to obtain the maximum re-dispersion efficiency, above which only a marginal improvement can be achieved. Therefore, the optimal conditions can be established in TMP_{sp} of

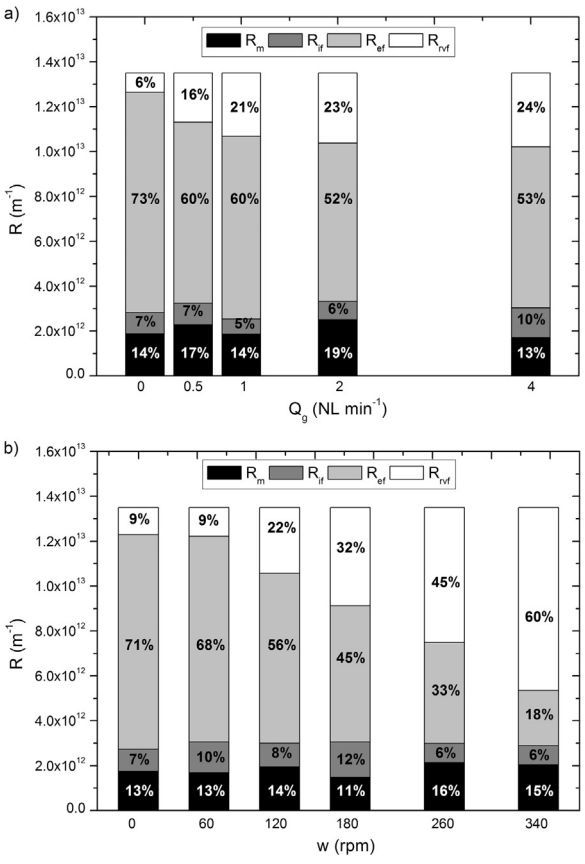

Fig. 4. Relative contribution of the different hydraulic resistances: clean membrane (R_m), internal residual fouling (Rif), external residual fouling (R_{ef}) and reversible fouling (Rrvf) against gas flowrate or rotating speed for (a) GS-HFM and (b) R-HFM. Pseudo-stationary zone; J=8 L/h m^2;J_B=30 L/h m^2;t_B=30 s; TMP_{sp}=30 kPa. All hydraulic resistances were calculated according to Eqs. (2)–(5).

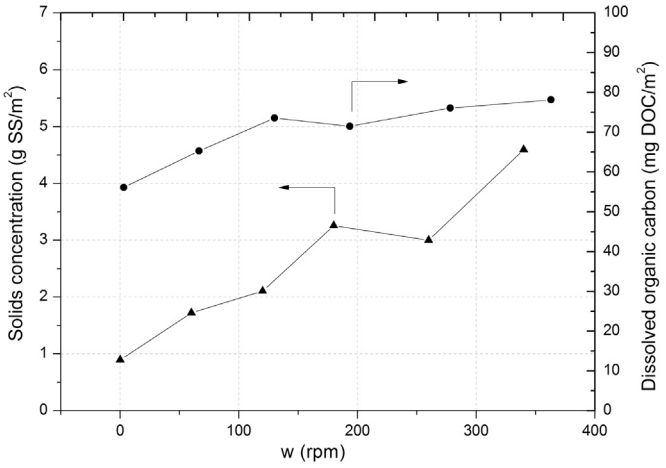

Fig. 5. Detached matter in terms of suspended solids (SS) and dissolved organic carbon (DOC) per membrane surface by the action of the backwashing with aid of membrane module rotation at different w.

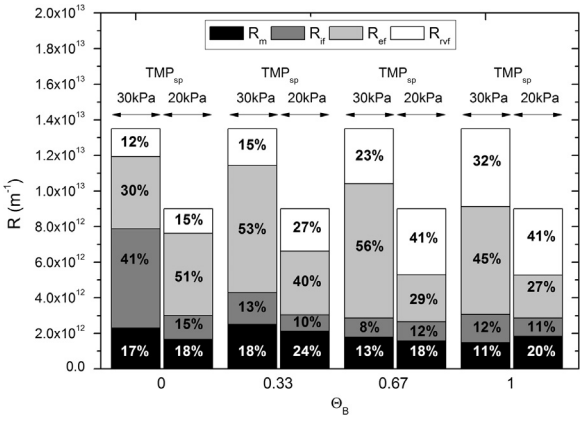

Fig. 6. Relative contribution of each resistance in the pseudo-stationary zone at two different TMP_{sp} and different Θ_B relationships. J=8 L/h m^2;J_B=30 L/h m^2; w=180 rpm; t_B+ t_R=30 s. All hydraulic resistances were calculated according to Eqs. (2)–(5).

20 kPa and Θ_B of 0.67 in terms of process productivity for the tested experimental unit and the given operational conditions (J, J_B, w, t_B+t_R). This was confirmed by analysis of the dispersed matter in the specific cleaning tests. Hence, Fig. 7 shows that higher values of dispersed TSS were obtained as Θ_B increased. In addition, roughly similar TSS were obtained for both TMP_{sp} at $\Theta_B \leq 0.67$, confirming that the maximum dispersion capability has been achieved at 0.67 for 20 kPa. On the other hand, results also revealed a minor role of the micro-colloidal and soluble fraction, expressed by the DOC values.

3.2. Continuous operation of the R-HFM as AnMBR

3.2.1. Filtration performance

Short-term tests have allowed to establish the best operation conditions for enhancing cake re-dispersion and thus, limiting the fouling phenomena. Nevertheless, the experimental unit was continuously essayed as bioreactor for more than 400 h in order to assess the feasibility of the process in long-term operation under conditions of expected compression and consolidation of cake [42]. TMP_{sp} was fixed at 20 kPa and Θ_B was established at 0.67, while permeate and backwashing fluxes of 8 and 30 L/h m^2, respectively, were applied.

Fig. 8a and b show the effect of three different rotating speeds (180, 260 and 340 rpm) on filtration performance, analysing the internal residual fouling and the net permeate flux. The net permeate flux, which quantifies the process productivity and takes into account the permeate losses during the backwashing and the cessation of filtration during the relaxation, was calculated by Eq. (7):

$$J_{net} = \frac{J \cdot t_F - J_B \cdot t_B}{t_F + t_B + t_R} \quad (7)$$

Concerning to internal residual fouling (R_{if}), which is related to the initial TMP at the beginning of each filtration cycle (Eq. (2)), the results showed a slight increase (from 1.6·10^{12} to 4.0·10^{12} m^{-1}, with R_m=1.6·10^{12} m^{-1}) during the first 20 h, followed by a stable and large period. This initial increase has been previously reported in other studies where the TMP_{sp} was used for physical cleaning initiation [8,43]. As previously mentioned, since cleaning only started when a fixed degree of fouling was reached (i.e. TMP_{sp}), this led to an extended filtration phase, which progressively decreased with subsequent cycles until the system reached equilibrium conditions. In this pseudo-stationary state, by considering the total hydraulic resistance at the TMP_{sp}, the relative contribution of the internal fouling resistance remained at a nearly constant value (17.5 ± 4.3%) regardless of the rotating speed applied. These results were only slightly higher to those previously obtained in short-term tests. Therefore, the long-term behaviour did not reveal any evidence of cake consolidation at tested conditions, suggesting that the system can be successfully operated during large periods. Nevertheless, further studies should be done in order to confirm the process sustainability with the R-HFM configuration at higher operating times, since some degree of biofouling could be formed as result of the deposition and growth of microorganisms on the membrane surface as Wang et al. reported [44].

A different trend was observed for the J_{net}, which abruptly decreased during the first 20 h of operation (from 7.5 to 4.3 L/h m^2). This net flux decline may be related to a progressive formation of an external residual layer. Consistently with results described in the previous sections, this type of fouling, caused a rapid cake re-deposition and represents the main determining factor on the duration of the filtration phase (i.e. the net permeate flux). Once the system reached pseudo-stationary state, the J_{net} stabilised at a value that depended on the rotating speed applied. Thus, average J_{net} values of 5.1 and 6.7 L/h m^2 were obtained as the speed increased to 260 and 340 rpm, respectively. It should be considered that even at the lowest speed, where the relative contribution of external residual fouling resistance was considerable (42.4 ± 1.8%), this external layer did not lead to a progressive consolidation process. Therefore, the membrane rotation, even at the lowest speed (180 rpm), should lead to process sustainability in large operation periods. In summary, these results confirmed the efficiency of the R-HFM for fouling control in severe conditions such as those comprising dead-end filtration and cleaning initiation by TMP_{sp}.

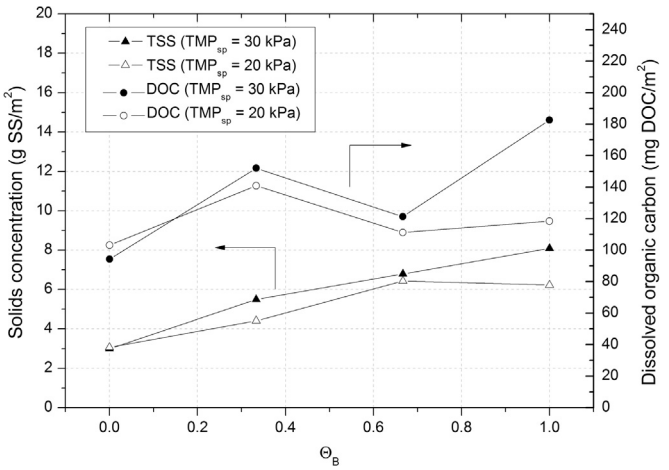

Fig. 7. Detached matter in terms of total suspended solids (TSS) and dissolved organic carbon (DOC) by the action of the backwashing with aid of membrane module rotation at different values of TMP_{sp} and Θ_B.

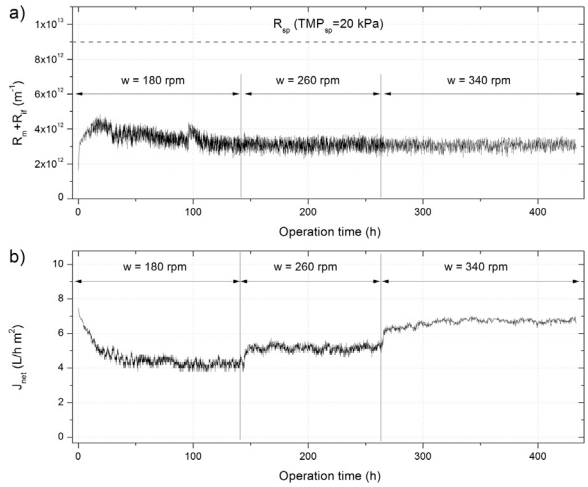

Fig. 8. Reported evolution of: (a) R_m+R_{if} with the elapsed time and (b) net flux (J_{net}) during long term tests. J=8 L/h m^2;J_B=30 L/h m^2;Θ_B=0.67; TMP_{sp}=20 kPa.

3.2.2. Biomass characteristics and treatment performance

Due to biomass properties can affect the filtration performance (i.e. membrane fouling), the objective of this subsection was to ensure that the bioreactor performance and the biomass properties remained stable during the long-term test. Table 3 summarises the main properties of the anaerobic suspension and the treatment performance along the long-term operation (Section 3.1.1), where the experimental unit set-up was modified to work as an AnMBR. Due to large values of HRT and SRT applied (31 h and complete retention, respectively), the system exhibited a stable behaviour, where the biomass concentration remained constant at 8.0 ± 0.9 g MLSS/L with a MLVSS/MLSS ratio of 78.9 ± 3.1%, indicating no significant accumulation of inorganic matter in the sludge. The suspension was characterised by low to median particle sizes (d_{50}=26.9 ± 1.5 μm) and high content of fine particles and colloids in the supernatant (supernatant turbidity=2085 ± 29 NTU). Consistently, the sludge showed poor filterability (TTF=11.0 ± 0.3 min). No significant differences were found in the pH, remaining close to neutral values (pH =7.5 ± 0.2). This was accompanied by alkalinity ratios below 0.3, suggesting that there is no accumulation of fatty acids.

Treatment performance was also evaluated through permeate quality. It can be observed a relatively low COD removal (65%), reaching effluent concentrations of 221 ± 54 mg/L, higher than typical values (100–120 mg/L) reported in other studies [45,46]. This discrepancy may be linked to the high soluble fraction of the feedwater (61%, see Table 1) and the psychrophilic conditions on the bioreactor (16.1 °C, on average), where microbial growth was greatly slowed, stretching out the time required for good acclimation. As expected for anaerobic processes, low nutrient removals and high sulphate reduction (85%) were also recorded.

3.2.3. Characterisation of the fouling layers

After the long-term operation (w=340 rpm) the membrane module was removed from the mixed-liquor and cleaned "ex-situ" following the cleaning protocol for fouling fractionation. Fig. 9 shows the different hydraulic resistances of the fouling fractions obtained at the end of each one of the physical (rinsed and extended backwashed) and chemical (NaOCl and citric acid desorption) cleaning steps of the "ex-situ" membrane cleaning protocol. Membrane cleaning contribution of each step was calculated by the relationship of the total hydraulic resistance associated to the TMP_{sp} (R_{sp}) and the values obtained by the subtracting of the successive resistances.

As expected from previous results, reversible fouling was the main contribution to total fouling (43.4%), which was effectively removed by the physical cleanings performed during the long-term test. At the end of the test, the hydraulic resistance of the fouled membrane was measured "ex-situ" in clean water, revealing that the overall contribution of the attached foulants (R_{if}+R_{ef}) was 35.2%. This value was similar to those reported during the short-term assays, confirming that there was not fouling consolidation. In general, it is accepted that the rinsed fraction was mainly composed of sludge flocs and biopolymers from the cake layer, while the extended backwashed fraction was mainly represented by the materials that blocked the membrane pores [38]. The use of both methods during the external physical cleaning protocol led to a solids removal of 99.3% (Fig. 10), reducing the hydraulic resistance at $3.5{\cdot}10^{12}$ m^{-1}. Also, the foulants that only can be removed by chemical means represented the internal residual fouling, which had an important contribution (17.3%). Unlike short-term assays where NaOCl was only needed to remove the organic foulants (mainly related to presence of a gel layer and macromolecule adsorption [44]), citric acid (usually associated with the presence of inorganic precipitates and scalants [6]) was also required in order to recover the initial membrane permeability.

In summary, the small contributions observed for the rinsed and extended backwashed fractions highlighted the effectiveness of the R-HFM configuration to remove the external fouling and to prevent cake consolidation.

4. Conclusions

A novel physical cleaning strategy based on membrane rotation has been studied at lab-scale to evaluate fouling removal. The effectiveness of this strategy combined with backwashing and relax was compared to the gas scouring conventional mode. In the present study the following may be concluded:

- Based on the resistances-in-series approach, external residual fouling has been identified as the main factor determining the process productivity. Shear stress promotion by membrane rotation during the backwashing phase can significantly enhance the re-dispersion of the detached foulants from the membrane surface to the bulk suspension, reducing the external fouling contribution (56–18%).
- Above Q_g values of 2 NL/min (SGD_m=0.3 Nm^3/h m^2) gas sparging re-dispersion efficiency was limited (53%) and no appreciable improvement of fouling control was observed.
- External residual fouling re-dispersion improved with the backwashing net ratio (Θ_B). On the other hand, an increase of the TMP_{sp} led to higher filtration phases and greater thickness of the cake layer, worsening foulants re-dispersion. Thus, in terms of process productivity the optimal conditions were found at TMP_{sp} and Θ_B values of 20 kPa and 0.67, respectively.
- Long-term test revealed the sustainability of the AnMBR operation

Table 3
Main properties of the anaerobic suspension and the treatment performance.

Parameter	Units	Mean ± sd
Suspension characterisation		
MLSS	g/L	8.0 ± 0.9
MLVSS	g/L	6.3 ± 0.7
MLVSS/MLSS	%	78.9 ± 3.1
TTF	min	11.0 ± 0.3
d_{50}	μm	26.9 ± 1.5
Supernatant turbidity	NTU	2085 ± 29
pH	–	7.5 ± 0.2
AI/AT	–	0.23 ± 0.07
Permeate quality		
COD	mg/L	221 ± 54
N-NH_3	mg/L	66.0 ± 7.4
PO_4^{3-}	mg/L	28.2 ± 4.8
SO_4^{2-}	mg/L	6.2 ± 2.3

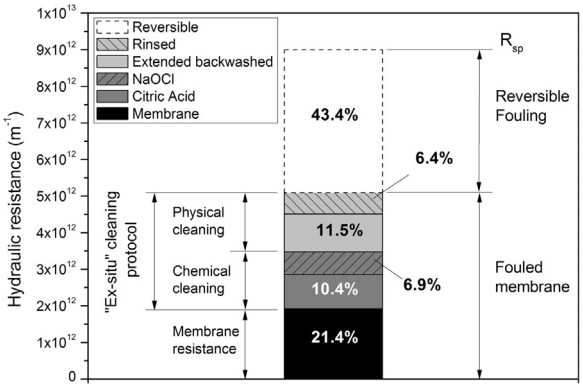

Fig. 9. Contribution to hydraulic resistances of the different foulants (after each one of the cleaning protocol steps) after the long-term assay.

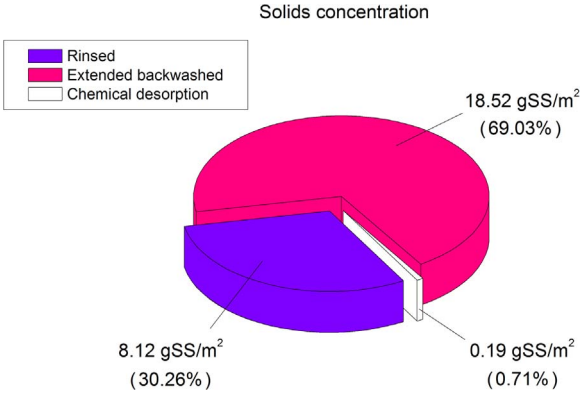

Fig. 10. Specific solid content per unit of membrane area in the resulting fractions from rinsed, backwashed and chemical desorption fractions. (In parentheses, the contribution as percentage is included).

during more than 400 h at a stable net permeate flux of 6.7 L/h m^2 when the rotating speed was fixed at 340 rpm.

Acknowledgments

This study has been carried out in the framework of MBRgenera-AGUA01 project funded by Fundación Cajacanarias (AGUA01). Mr Ignacio Ruigómez wishes express his gratitude for the support of the FPI Grant Program of the MINECO (BES-2012–060920) associated to the national research project CTM2011-27307. The authors are grateful to the Tenerife Water Council and the Northeast Wastewater Treatment Plant for supplying water and sludge and their collaboration in pilot plant implementation. Also, analytical advice of the Water Analysis Laboratory of the ULL Chemical Engineering Department has been essential for the development of this work.

References

[1] A. Smith, L. Stadler, N. Love, S. Skerlos, L. Raskin, Perspectives on anaerobic membrane bioreactor treatment of domestic wastewater: a critical review, Bioresour. Technol. 122 (2012) 149–159.
[2] H. Ozgun, R.K. Dereli, M.E. Ersahin, C. Kinaci, H. Spanjers, J.B. van Lier, A review of anaerobic membrane bioreactors for municipal wastewater treatment: integration options, limitations and expectations, Sep. Purif. Technol. 118 (2013) 89–104.
[3] C. Visvanathan, A. Abeynayaka, Developments and future potentials of anaerobic membrane bioreactors (AnMBRs), Membr. Water Treat. 3 (2012) 1–23.
[4] D. Stuckey, Recent developments in anaerobic membrane reactors, Bioresour. Technol. 122 (2012) 137–148.
[5] D.J. Batstone, T. Hülsen, C.M. Mehta, J. Keller, Platforms for energy and nutrient recovery from domestic wastewater: a review, Chemosphere 140 (2015) 2–11.
[6] S. Judd, The MBR Book: Principles and Applications of Membrane Bioreactors for water and Wastewater Treatment, second edition (2011), 2011.
[7] Y. Ye, V. Chen, P. Le-Clech, Evolution of fouling deposition and removal on hollow fibre membrane during filtration with periodical backwash, Desalination 283 (2011) 198–205.
[8] L. Vera, E. González, I. Ruigómez, J. Gómez, S. Delgado, Analysis of backwashing efficiency in dead-end hollow-fibre ultrafiltration of anaerobic suspensions, Environ. Sci. Pollut. Res. 22 (2015) 16600–16609.
[9] A. Drews, Membrane fouling in membrane bioreactors - Characterisation, contradictions, cause and cures, J. Membr. Sci. 363 (2010) 1–28.
[10] L. Vera, E. González, O. Díaz, R. Sánchez, R. Bohorque, J. Rodríguez-Sevilla, Fouling analysis of a tertiary submerged membrane bioreactor operated in dead-end mode at high-fluxes, J. Membr. Sci. 493 (2015) 8–18.
[11] D. Jeison, J.B. van Lier, Cake formation and consolidation: main factors governing the applicable flux in anaerobic submerged membrane bioreactors (AnSMBR) treating acidified wastewaters, Sep. Purif. Technol. 56 (2007) 71–78.
[12] C. Ramos, A. García, V. Diez, Performance of an AnMBR pilot plant treating high-strength lipid wastewater: biological and filtration processes, Water Res. 67 (2014) 203–215.
[13] David Martinez-Sosa, Brigitte Helmreich, Harald Horn, Anaerobic submerged membrane bioreactor (AnSMBR) treating low-strength wastewater under psychrophilic temperature conditions, Process Biochem. 47 (2012) 792–798.
[14] S.P. Hong, T.H. Bae, T.M. Tak, S. Hong, A. Randall, Fouling control in activated sludge submerged hollow fiber membrane bioreactors, Desalination 143 (2002) 219–228.
[15] J.B. Giménez, A. Robles, L. Carretero, F. Durán, M.V. Ruano, M.N. Gatti, J. Ribes, J. Ferrer, A. Seco, Experimental study of the anaerobic urban wastewater treatment in a submerged hollow-fibre membrane bioreactor at pilot scale, Bioresour. Technol. 102 (2011) 8799–8806.
[16] A. Kola, Y. Ye, P. Le-Clech, V. Chen, Transverse vibration as novel membrane fouling mitigation strategy in anaerobic membrane bioreactor applications, J. Membr. Sci. 455 (2014) 320–329.
[17] G. Ferrero, I. Rodriguez-Roda, J. Comas, Automatic control systems for submerged membrane bioreactors: a state-of-the-art review, Water Res. 46 (2012) 3421–3433.
[18] L. Vera, E. González, I. Ruigómez, J. Gómez, S. Delgado, Influence of gas sparging intermittence on ultrafiltration performance of anaerobic suspensions, Ind. Eng. Chem. Res. 55 (2016) 4668–4675.
[19] R. Villarroel, S. Delgado, E. González, M. Morales, Physical cleaning initiation controlled by transmembrane pressure set-point in a submerged membrane bioreactor, Sep. Purif. Technol. 104 (2013) 55–63.
[20] Z.F. Cui, S. Chang, A.G. Fane, The use of gas bubbling to enhance membrane processes, J. Membr. Sci. 221 (2003) 1–35.
[21] Lijun Xia, Adrian Wing-Keung Law, Anthony G. Fane, Hydrodynamic effects of air sparging on hollow fiber membranes in a bubble column reactor, Water Res. 47 (2013) 3762–3772.
[22] T. Ueda, K. Hata, Y. Kikuoka, O. Seino, Effects of aeration on suction pressure in a submerged membrane bioreactor, Water Res. 31 (1997) 489–494.
[23] F. Meng, S. Chae, A. Drews, M. Kraume, H. Shin, F. Yang, Recent advances in membrane bioreactors (MBRs): membrane fouling and membrane material, Water Res. 43 (2009) 1489–1512.
[24] S.Z. Abdullah, H.E. Wray, P.R. Bérubé, R.C. Andrews, Distribution of surface shear stress for a densely packed submerged hollow fiber membrane system, Desalination 357 (2015) 117–120.
[25] H. Husain, P. Côté, Membrane bioreactors for municipal wastewater treatment, Water Qual. Int. (1999) 19–22.
[26] T. Jiang, H. Zhang, D. Gao, F. Dong, J. Gao, F. Yang, Fouling characteristics of a novel rotating tubular membrane bioreactor, Chem. Eng. Process. 62 (2012) 39–46.
[27] I. Ruigómez, L. Vera, E. González, G. González, J. Rodríguez-Sevilla, A novel rotating HF membrane to control fouling on anaerobic membrane bioreactors treating wastewater, J. Membr. Sci. 501 (2016) 45–52.
[28] T.J. Rector, J.L. Garland, S.O. Starr, Dispersion characteristics of a rotating hollow fiber membrane bioreactor: effects of module packing density and rotational frequency, J. Membr. Sci. 278 (2006) 144–150.
[29] I. Ruigómez, L. Vera, E. González, J. Rodríguez-Sevilla, Pilot plant study of a new rotating hollow fibre membrane module for improved performance of an anaerobic submerged MBR, J. Membr. Sci. 514 (2016) 105–113.
[30] Z. Huang, S.L. Ong, H.Y. Ng, Submerged anaerobic membrane bioreactor for low-strength wastewater treatment: effect of HRT and SRT on treatment performance and membrane fouling, Water Res. 45 (2011) 705–713.
[31] S. Delgado, R. Villarroel, E. González, Effect of the shear intensity on fouling in submerged membrane bioreactor for wastewater treatment, J. Membr. Sci. 311 (2008) 173–181.
[32] I. Martin Garcia, M. Mokosch, A. Soares, M. Pidou, B. Jefferson, Impact on reactor configuration on the performance of anaerobic MBRs: treatment of settled sewage in temperate climates, Water Res. 47 (2013) 4853–4860.
[33] J. Gouveia, F. Plaza, G. Garralon, F. Fdz-Polanco, M. Peña, A novel configuration for an anaerobic submerged membrane bioreactor (AnSMBR). Long-term treatment of municipal wastewater under psychrophilic conditions, Bioresour. Technol. 198 (2015) 510–519.
[34] R. Pretel, A. Robles, M.V. Ruano, A. Seco, J. Ferrer, The operating cost of an anaerobic membrane bioreactor (AnMBR) treating sulphate-rich urban wastewater, Sep. Purif. Technol. 126 (2014) 30–38.
[35] Standard Methods for the examination of Water and Wastewater, 21st ed. American Public Health Association/Water Environment Federation, Washington DC USA, 2005.
[36] L. Ripley, W. Boyle, J. Converse, Improved alkalimetric monitoring for anaerobic digestion of high strength wastes, J. Water Pollut. Control Fed. 58 (1986) 406–411.
[37] J.A. Villamil, V.M. Monsalvo, J. Lopez, A.F. Mohedano, J.J. Rodriguez, Fouling control in membrane bioreactors with sewage-sludge based adsorbents, Water Res.

105 (2016) 65–75.
[38] J. Wu, P. Le-Clech, R.M. Stuetz, A.G. Fane, V. Chen, Effects of relaxation and backwashing conditions on fouling in membrane bioreactor, J. Membr. Sci. 324 (2008) 26–32.
[39] B.G. Fulton, J. Redwood, M. Tourais, P.R. Bérubé, Distribution of surface shear forces and bubble characteristics in full-scale gas sparged submerged hollow fiber membrane module, Desalination 281 (2011) 128–141.
[40] E.J. McAdam, E. Cartmell, S.J. Judd, Comparison of dead-end and continuous filtration conditions in a denitrification membrane bioreactor, J. Membr. Sci. 369 (2011) 167–173.
[41] P. Gui, X. Huang, Y. Chen, Y. Qian, Effect of operational parameters on sludge accumulation on membrane surfaces in a submerged membrane bioreactor, Desalination 151 (2003) 185–194.
[42] V. Diez, D. Ezquerra, J.L. Cabezas, A. García, C. Ramos, A modified method for evaluation of critical flux, fouling rate and in situ determination of resistance and compressibility in MBR under different fouling conditions, J. Membr. Sci. 453 (2014) 1–11.
[43] L. Vera, E. González, O. Díaz, S. Delgado, Application of a backwashing strategy based on transmembrane pressure set-point in a tertiary submerged membrane bioreactor, J. Membr. Sci. 470 (2014) 504–512.
[44] Z. Wang, J. Ma, C.Y. Tang, K. Kimura, Q. Wang, X. Han, Membrane cleaning in membrane bioreactors: a review, J. Membr. Sci. 468 (2014) 276–307.
[45] A. Robles, M.V. Ruano, J. Ribes, J. Ferrer, Performance of industrial scale hollow-fibre membranes in a submerged anaerobic MBR (HF-SAnMBR) system at mesophilic and psychrophilic conditions, Sep. Purif. Technol. 104 (2013) 290–296.
[46] J. Gouveia, F. Plaza, G. Garralon, F. Fdz-Polanco, M. Peña, Long-term operation of a pilot scale anaerobic membrane bioreactor (AnMBR) for the treatment of municipal wastewater under psychrophilic conditions, Bioresour. Technol. 185 (2015) 225–233.